Measurement of the Abraham Force in a Barium Titanate Specimen

G. B. WALKER, D. G. LAHOZ[1], AND G. WALKER
Department of Electrical Engineering, University of Alberta, Edmonton 7, Alberta

Received February 28, 1975

Accurate measurements of the Abraham density force have been conducted in a $BaTiO_3$ ceramic for the first time. The measured torque amplitudes (in the order of 10^{-10} Nm) were in good agreement with the predicted values inside the error limits of 10%. This conclusively rules out Minkowski's unsymmetric momentum-energy tensor for material media at low frequencies.

On a effectué pour la première fois des mesures précises de la densité de force Abraham dans une céramique $BaTiO_3$. Les amplitudes de couple mesurées (de l'ordre de 10^{-10} Nm) sont en bon accord avec les valeurs prédites, à l'intérieur des limites d'erreur de 10%. Ce résultat exclut de façon définitive l'emploi du tenseur d'énergie-impulsion non symétrique de Minkowski pour les basses fréquences dans les milieux matériels.

[Traduit par le journal]

Can. J. Phys., 53, 2577 (1975)

Introduction

The problem of ascertaining the mechanical force density inside a material medium due to the presence of an electromagnetic field has never been resolved and has been the subject of controversy among leading authorities (Pauli 1958). No disagreement exists in regard to the mechanical force on electric charge in free space or on the static overall translational force on a material body surrounded by free space. In such situations the four-divergence of the momentum-energy tensor provides the same result despite differences in the form of that tensor. There are two basic forms, one given by Minkowski (1908) and the other by Einstein and Laub (1908) which was later modified by Abraham (1909). From a practical point of view, the significant difference, as discussed by Marx and Gyorgyi (1954), is that the Abraham tensor predicts a force density f in an isotropic material medium given by:

$$[1] \qquad f = \frac{(\varepsilon_r\mu_r - 1)}{c^2}\frac{\partial}{\partial t}(E \times H)$$

which must be 'added' to the one of Minkowski (Brevik 1970).[2] Of the many attempts to settle this question by experiment, the most important so far appears to be that reported in a Ph.D. thesis by James (1968) which has recently come to the authors' attention. Measurements were performed at a frequency of about 3 kHz in a ferromagnetic material, ponderomotive forces being detected by a piezoelectric crystal. The theory of James' experiment is quite complicated but results clearly show that the Minkowski expression does not adequately represent the actual forces.

The experiment to be described here was first reported by Walker and Lahoz (1975) and has since been improved. It is relatively simple in experimental details and gives results which can easily be verified. Perhaps the most important feature is that electrostriction and other phenomena associated with electromagnetic fields in material media do not give any contribution to the measured torque. Our experiment was conducted at a frequency of about 0.3 Hz and is restricted to the special case of time varying E and fixed H in a nonmagnetic dielectric. Although no conclusions in regard to higher (*e.g.*, optical) frequencies are drawn, the inadequacy of the Minkowski tensor is clearly demonstrated.

Theory of Experiment

The experiment was performed by suspending a disk of high dielectric constant (barium titanate) as a torsional pendulum. The suspension was a thin tungsten fiber and the disk was located between the pole pieces of a powerful electromagnet. The apparatus is shown diagrammatically in Fig. 1. The movement of the disk was observed by reflecting a laser beam from a small mirror attached to the disk. The light beam had an arm length of 10 m and was compacted by a system of mirrors so that the final scale was close to and integral with the

[1]Present address: Department of Physics, University of Alberta, Edmonton, Alberta.

[2]This paper contains an extensive bibliography on the topic.

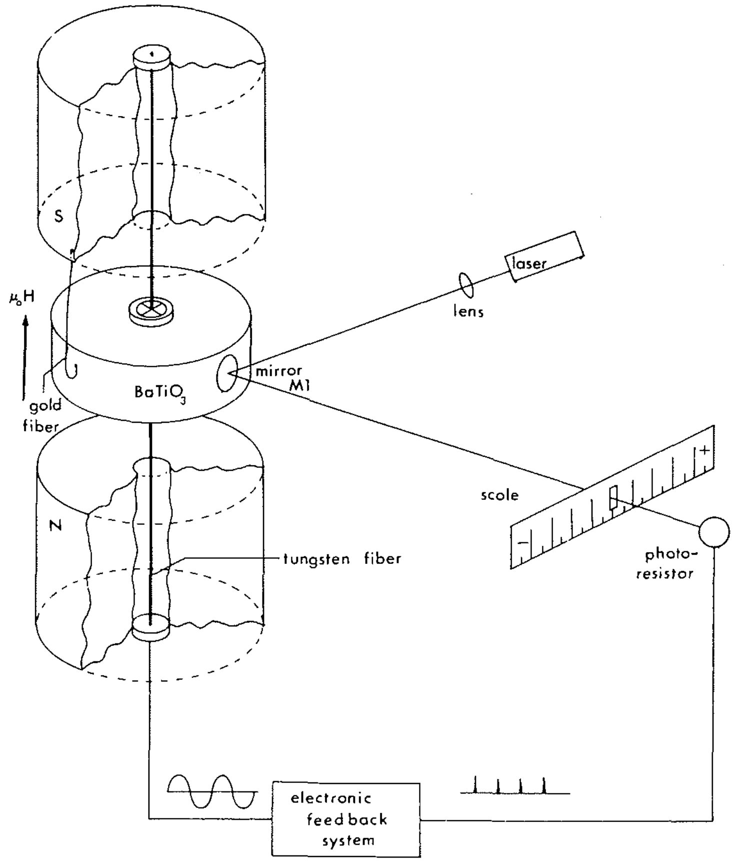

FIG. 1. Diagram of the experimental apparatus.

entire equipment. An important feature was the use of a light sensitive cell located on the final scale to generate, by means of electronic circuits, a sinusoidal voltage which was of the exact periodicity of the pendulum and could be applied across the disk in any desired phase.

The disk had a central hole and the outer and inner cylindrical surfaces were coated with a layer of aluminum sufficient to give good conductivity. The outer surface was connected to ground (a magnet pole piece) by means of a thin gold fiber located parallel to the magnetic field and the inner connected to the supporting tungsten fiber. The mechanical torque produced by current in the gold fiber and in the connection to the tungsten fiber was less than 0.5% of the torque to be measured.

The electric field in the disk is

$$[2] \qquad E(r) = V/(r \ln (r_2/r_1))$$

where V is the voltage across the disk and r_1 and r_2 the inner and outer radii respectively. The torque in an annular ring of radius r and width dr is

$$[3] \qquad \mathrm{d}T = -2\pi\theta \frac{\varepsilon_r\mu_r - 1}{c^2} H \frac{\partial E(r)}{\partial t} r^2 \,\mathrm{d}r$$

where θ is the disk thickness. Assuming the applied voltage to be given by $V = -V_0 \cos(\omega t + \phi)$, the torque on the disk, by simple integration, is

$$[4] \qquad T = -T_0 \sin(\omega t + \phi)$$

with

$$[5] \qquad \frac{T_0}{\omega} = \pi\varepsilon_0(\varepsilon_r\mu_r - 1)\theta(\mu_0 H) V_0 \frac{r_2{}^2 - r_1{}^2}{\ln(r_2/r_1)}$$

Let I, δ, and γ be respectively the inertia moment, damping factor, and elastic constant of the torsional pendulum. Then the angular position α of the mirror attached to the specimen satisfies

[6] $$T = I(\mathrm{d}^2\alpha/\mathrm{d}t^2) + \delta(\mathrm{d}\alpha/\mathrm{d}t) + \gamma\alpha = -T_0 \sin(\omega t + \phi)$$

If the resonant frequency, $\omega_0 \equiv \sqrt{(\gamma/I) - (\delta^2/4I^2)}$, of the torsional pendulum is 'identical' to the frequency ω of the impressed torque and if the 'Q' of this mechanical system, $Q \equiv \gamma/\delta\omega$, is very large, then the general solution of [6] can be written:

[7] $$\alpha(t) = F\,\mathrm{e}^{-t/\tau} \sin(\omega t + \sigma) + (T_0/\delta\omega)[\cos(\omega t + \phi) + O(Q^{-1})]$$

where F and σ are the integration constants and τ, the time constant, is defined by $\tau = 2I/\delta$.

Terms like the last one in [7] will be omitted because in our system the 'Q' was greater than 1000. This 'Q' can obviously be expressed in many different ways:

[8] $$Q \equiv \gamma/\delta\omega = I\omega/\delta = (1/2)\tau\omega$$

If the initial conditions are $\alpha(0) = \alpha_0$, $\alpha'(0) = 0$, then the general solution [7] becomes:

[9] $$\alpha = (T_0/\delta\omega)\cos(\omega t + \phi)[1 - \mathrm{e}^{-t/\tau}] + \alpha_0 \cos\omega t\, \mathrm{e}^{-t/\tau}$$

In order to predict the actual behavior of the time variation of the swinging spot on the scale, it is necessary to obtain the envelope of the peaks of [9] defined by $\mathrm{d}\alpha/\mathrm{d}t = 0$, *i.e.* by

[10] $$-(T_0/\delta)\sin(\omega t + \phi)[1 - \mathrm{e}^{-t/\tau}] - \alpha_0\omega \sin\omega t\, \mathrm{e}^{-t/\tau} = 0$$

This equation has the solution $\omega t/\pi$ = integer for either $\phi = 0$ or $\phi = \pi$ and this is all that is needed because these two restrictions correspond respectively to the following significant cases: (*a*) the 'in phase' situation, $\phi = 0$, and (*b*) the 'antiphase' situation, $\phi = \pi$, which is achieved when only the voltage or, alternatively, the magnetic field is changed in sign. Consequently, the envelopes of the positive peaks of [9] are:

[11] $$\hat{\alpha}(t) = \alpha_0\, \mathrm{e}^{-t/\tau} + (T_0/\delta\omega)(1 - \mathrm{e}^{-t/\tau}) \quad \text{for } \phi = 0$$

[12] $$\hat{\alpha}(t) = \alpha_0\, \mathrm{e}^{-t/\tau} - (T_0/\delta\omega)(1 - \mathrm{e}^{-t/\tau}) \quad \text{for } \phi = \pi$$

By allowing $T_0 = 0$ in [9] and [12], the unforced solution of the pendular motion and its envelope are, respectively, obtained:

[13, 14] $$\alpha(t) = \alpha_0 \cos\omega t\, \mathrm{e}^{-t/\tau}; \quad \hat{\alpha}(t) = \alpha_0\, \mathrm{e}^{-t/\tau}$$

Summarizing one can say that the observable effect of the torque consists in shifting the unforced envelope [14] positively or negatively (for $\phi = 0$, $\phi = \pi$ respectively) by an amount

[15] $$(T_0/\delta\omega)(1 - \mathrm{e}^{-t/\tau}) = \alpha(\infty)(1 - \mathrm{e}^{-t/\tau})$$

This is represented in Fig. 2.

The light beam striking the moving mirror experiences a peak deflection $2\hat{\alpha}$. For an optical arm length R, the total peak to peak swing of the reflected laser beam falling on the scale is given by $A = 2 \times 2 \times R \times \hat{\alpha}$. The expected quantities to be measured, after normalizing to the initial value $A(0)$, are:

[16] $$A^+(t)/A(0) = \mathrm{e}^{-t/\tau} + (A(\infty)/A(0))(1 - \mathrm{e}^{-t/\tau}) \quad \text{for } \phi = 0$$

[17] $$A^-(t)/A(0) = \mathrm{e}^{-t/\tau} - (A(\infty)/A(0))(1 - \mathrm{e}^{-t/\tau}) \quad \text{for } \phi = \pi$$

[18] $$A^\circ(t)/A(0) = \mathrm{e}^{-t/\tau} \quad \text{for } T_0 = 0$$

with $A(\infty) = 4R\alpha(\infty)$ or more explicitly, after collecting together [15], [5], and [8]:

[19] $$A(\infty) = 4R\frac{T_0}{2\omega I/\tau} = 2\pi\theta\frac{r_2^{\,2} - r_1^{\,2}}{\ln(r_2/r_1)} R\frac{\tau}{I}\varepsilon_0(\varepsilon_r\mu_r - 1)(\mu_0 H)V_0$$

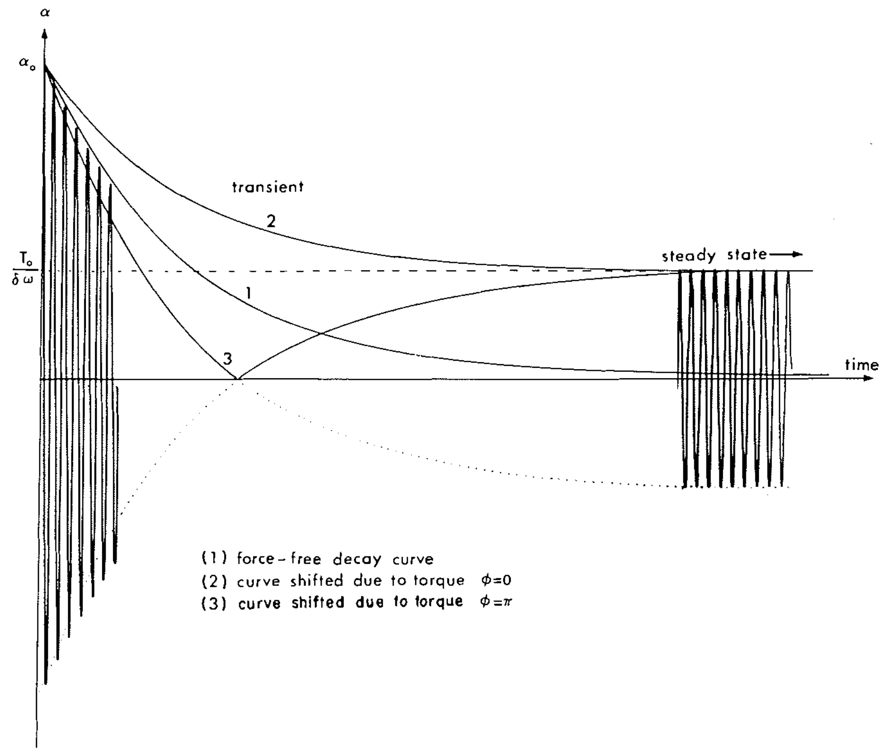

FIG. 2. Effect of the torque on the exponential decay.

For a given moment of inertia I, where I is $(1/2)\pi\rho_m\theta(r_2^{\ 4} - r_1^{\ 4})$ and ρ_m = mass density, it is interesting to note that, from [19], if the fields, τ and ρ_m can be specified independently, a rodlike geometry for the specimen would actually give a higher value of $A(\infty)$ than the disk shape used.

It is very remarkable that the steady state amplitude, $A(\infty)$, does not depend explicitly on the frequency of operation $\omega/2\pi$. This can be used to obtain the required sensitivity of the system. It is well known that the internal friction of a given twisting metallic fiber (Zener 1948) is a complex oscillating function of the frequency with characteristic minimums depending on the crystalline structure. A rough theoretical approach, however, can be obtained assuming that the internal friction of a twisting metallic fiber (Fig. 3) is similar to that of a column of viscous fluid. Then

$$[20] \qquad dT_f = r\eta(\Delta v/\Delta l)\,ds$$

with dT_f = incremental friction torque; r = radius of the surface element ds; $ds = 2\pi r\,dr$; η = viscosity coefficient (constant?); and l = length of the fiber. $\Delta v/\Delta l$ represents the gradient

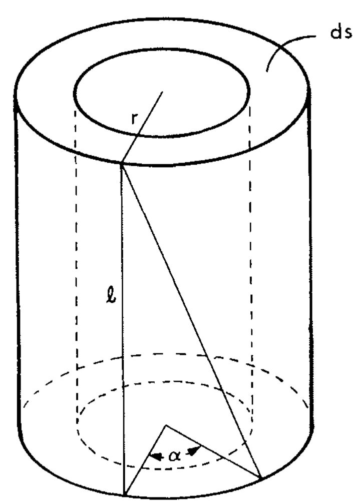

FIG. 3. Fiber model.

of relative velocity between two corresponding surface elements, ds. Now assume $\Delta v/\Delta l \simeq v/l = (r/l)(d\alpha/dt)$ to integrate [20] for the complete cross section of the fiber of radius a:

$$[21] \qquad T_f = \frac{2\pi\eta}{l}\frac{d\alpha}{dt}\int_0^a r^3\,dr = \frac{\pi\eta}{2}\frac{a^4}{l}\frac{d\alpha}{dt}$$

A comparison with [6] gives a (theoretical) damping factor, $\delta = (\pi\eta/2)(a^4/l)$. This relationship can be expressed in terms of the time constant, τ, and the frequency ω of the torsional pendulum by means of [8]: If G is the rigidity of the fiber then

$$[22] \qquad \tau = 2G/\eta\omega^2 = \text{constant}/\omega^2$$

Experimentally we have found, with tungsten fibers in the region of 1 Hz, that τ was roughly proportional to ω^{-n} with $1 < n < 2$. Anyway, it is clear that τ (and, consequently, the sensitivity of the system) can easily be increased by lowering the frequency of operation $\omega/2\pi$. The τ was also enhanced by a factor of 2 to 4 by placing the torsional pendulum in a 10^{-5} Torr vacuum chamber; however, this did add complexity to the system. Although under best conditions we were able to obtain values of τ up to 2 h, the usual mechanical noise acting on the system restricted τ to a practical maximum of about 65 min.

Another important point must be mentioned in connection with the low frequency of operation. The current flowing in the disk has two components in quadrature, the displacement current and the effective conduction current. Thus, if the applied voltage is exactly in phase (or in antiphase) with the mechanical oscillation of the pendulum, the mechanical force due to the polarization current interacting with the magnetic field will assist (or diminish) the oscillation, whereas the effect on the pendulum of the forces due to conduction currents are self-cancelling.[3] This is a most helpful consideration but it must be noted that unavoidable small fluctuations in the oscillation of the disk are not accurately reproduced in the applied voltage and, hence, a resultant effect due to the conduction current will occur. This could be objectionable if the frequency were so low that the conduction currents become comparable with the displacement current. Consequently, the impedance of the ceramic condenser has to be substantially reactive, $\varepsilon\rho\omega \geq 1$, ρ being the resistivity. For our specimen of $BaTiO_3$ the resistance measured between the coated cylindrical surfaces was 2.4×10^{12} Ω and the corresponding capacitance was about 2×10^{-3} μF. In the region of 0.5 Hz this gives $\rho\varepsilon\omega = RC\omega > 10^4$; thus, the aforesaid requirements were more than adequately complied with.

[3]The conduction current is in phase with the applied voltage, whereas the polarization current is in time quadrature. Thus, if the phase of the applied voltage is synchronized with the oscillations of the pendulum so that the polarization current is in phase (or in antiphase) with the pendulum, the Lorentz force due to conduction current will assist the motion of the pendulum in one quarter cycle and oppose in the next quarter cycle. It is thus self-cancelling over each complete cycle.

Description of the Experimental System

The geometry of the torsional pendulum may be visualized from Fig. 1. However, the magnitude of the density force to be observed necessitated careful selection of the suspension system both for the disk itself and for the complete system. The $BaTiO_3$ ceramic was securely clamped to the 0.2 mm tungsten fiber by the brass compression nut forming part of the central conductor of the disk. A Varian VA4005 electromagnet with adjustable pole pieces provided the axial field: The poles had a 1 cm diameter hole drilled along the axis to pass the tungsten fiber which was then rigidly clamped into insulated feed-throughs mounted on the outside faces of the cylindrical pole pieces. Each pole piece was 27 cm long and with a magnet gap of 3.9 cm; the effective length of the fiber on each side of the ceramic was 29 cm. The lower feed-through was a commercial vacuum type and provided the electrical contact to the inner conductor of the disk. The upper feed-through was machined out of plexiglass with a threaded brass rod connected to the fiber in order that tension could be applied to this tungsten fiber from outside the vacuum. Apiezon Q compound provided an adequate vacuum seal. The vacuum chamber consisted of a 5 cm long section of 9 cm copper tubing with 'O' rings located between the copper and the pole faces. One port of the vacuum chamber led through a valve to a pair of Varian sorption pumps for roughing the vacuum chamber and a second port was connected to the Varian 8 l/s vacion pump for pumping of the system to the necessary 10^{-5} Torr. The sorption pump section was detached from the system once roughing was completed to eliminate any vibration effects during the experiments. The front portion of the copper chamber was cut away and replaced with a removable plexiglass section fitted with a glass window to transmit the laser beam.

Two tables, each 1.52 m × 0.76 m and 0.81 m high, were bolted end to end and strengthened beneath the tops by two 3 m lengths of I beam.

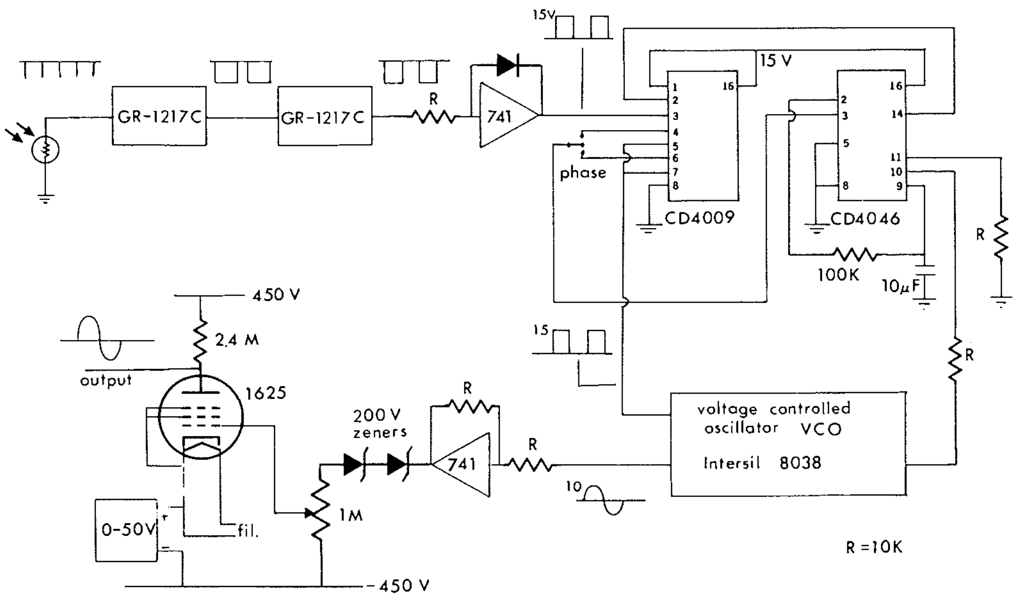

FIG. 4. Feedback system.

To isolate the system from ambient noise the entire structure was suspended from the ceiling of a high bay laboratory by a 5 ton chain hoist. Steel cables ran from the tables to a 2.4 m length of steel beam which in turn was suspended from the hoist by 3 m of chain with an automobile tire as an additional damping element. To balance the weight of the electromagnet and to increase the inertia of the table itself, 12 concrete blocks were placed at the other end of the tables. Located on the blocks was the optical system consisting of the laser source, three mirrors to multiply the length of the light path, and the calibrated centimetric scale. The total weight of the suspended system was 800 kg.

The electronic portion of the system is shown in the schematic diagram of Fig. 4. Basically it provides a low frequency high voltage sinusoidal signal phase locked to the mechanically oscillating torsional system. The photoresistor located in the center of the centimetric scale at the end of the light path responds each time the laser spot passes. The resulting voltage pulse triggers a pulse generator which acts as a monostable multivibrator giving one pulse per cycle. A second pulse generator provides a symmetrical square wave in phase with the input pulses. The voltage controlled oscillator (VCO) is then phase locked to this square wave by using the phase detector and amplifier portions of a standard phase locked loop integrated circuit (CD4046AE). The sinusoidal output of the oscillator is amplified to 500 V (p.p.) using a 1625 pentode and suitable level shifting circuitry. By using inverters in the phase-lock circuit, the phase of the output voltage may be switched to 180° with respect to the input pulse. Final phase adjustment is accomplished using the frequency control of the VCO. The period of the mechanical system and, hence, of the electronic system was ~4 s; however, the phase lock acquisition time was only about three periods. A storage oscilloscope was used to monitor the driving voltage and to compare the phase with respect to the input pulses.

System Parameters

Equation 19 can be rewritten as follows:

$$[23] \qquad T_0^{\mathrm{obs}} = (A(\infty)I/2R\tau)\omega$$

The right member can be considered as the Abraham torque to be measured; whereas the predicted torque, from [19], is

$$[24] \quad T_0^{\mathrm{calc}} = \pi\varepsilon_0(\varepsilon_r\mu_r - 1) \times (\mu_0 H)\theta V_0 \frac{r_2^2 - r_1^2}{\ln(r_2/r_1)}\omega$$

Safely assuming $\mu_r = 1$, in order to compare [23] with [24], one therefore needs to measure

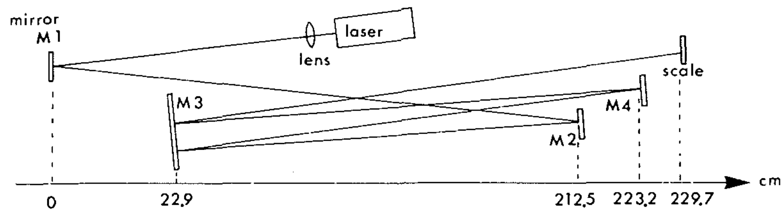

FIG. 5. Optical path.

ten quantities: R, θ, r_2, r_1, I, ε_r, $\mu_0 H$, V_0, τ, and $A(\infty)$. Let us start by specifying the first six, which may be termed the structural parameters of the system, since they were kept constant in the course of the experiment.

(a) Optical Arm, R

The path of the laser beam is shown in Fig. 5. The optical arm consequently had a total measured length of $R = (1010 \pm 5)$ cm.

(b) Ceramic Dimensions

The dimensions of the specimen, machined in the form of a cylindrical condenser, could be determined with negligible error: thickness, $\theta = (1.988 \pm 0.001)$ cm; external radius, $r_2 = (2.630 \pm 0.001)$ cm; internal radius, $r_1 = (0.3975 \pm 0.001)$ cm.

(c) Inertial Moment, I

The simple geometry of the disk allowed an easy calculation of the inertial moment: $I = (1/2)M(r_2^2 + r_1^2) + 9.9$ gcm^2. The last term represents the estimated contribution of the two small circular mirrors diametrically opposed on the surface of the disk. The mass M being (217.5 ± 0.1) g, the result is $I^{\text{calc}} = (779 \pm 10)$ gcm^2, where the wide error margin is primarily due to uncertainty in the volume of the small brass compression clamp used to attach the ceramic to the tungsten fiber. In order to reduce this error, a dynamical method was also used: An accurately machined brass ring with well determined inertia moment, $\hat{I} = (323.1 \pm 1)$ gcm^2, could be fitted on the oscillating ceramic disk. The two different periods were measured with high precision: $T = 2.6773$ s and $T' = 3.1844$ s. Then the 'measured' inertia moment of the disk is given by

$$I^{\text{meas}} = \hat{I}\,\frac{T^2}{(T' - T)(T' + T)} = (779.2 \pm 4)\ \text{gcm}^2$$

and is in excellent agreement with the calculated value.

(d) Dielectric Constant, ε_r

A low frequency impedance bridge gave an accurate determination of the capacitance between the two coated surfaces of the dielectric. It increased from 2.11 nF at 5 Hz to 2.12 nF at 0.5 Hz near the intended operation frequency. One can obviously neglect the field fringing effects for a condensor of extremely high permittivity. Taking $C = (2.12 \pm 0.01)$ nF, the value of the dielectric constant is therefore obtained as follows:

$$\varepsilon_r = \frac{C \ln (r_2/r_1)}{2\pi\varepsilon_0\theta} = 3620 \pm 15$$

(e) Magnetic Field $\mu_0 H$ and Voltage Amplitude, V_0

The maximum magnetic field was measured both by a calibrated induction gaussmeter and by the bismuth resistance method. Due to a small difference in the shape of the pole pieces of the electromagnet, the magnetic field lines diverged slightly from the top pole towards the bottom: However, in the region of the ceramic the field lines were reasonably uniform. The utilized (mean) value was $\mu_0 H_{\text{max}} = (0.97 \pm 0.02)$ Wb m^{-2}. The magnetic field could be adjusted by changing the coil current but in practice only four settings were used: $\pm\mu_0 H_{\text{max}}$ and $\pm 0.8\,\mu_0 H_{\text{max}}$.

The values of applied voltage used are indicated in Table 1 and were measured with an oscilloscope to within $\pm 3\%$. In excess of 550 V (p.p.) the electrostatic charge formed on the ceramic produced significant forces which perturbed the system. At this value, also, nonlinearity of the output stage resulted in distortion of the sinusoidal waveform. Consequently, these two considerations dictated the maximum useful voltage.

A comment may be made regarding error resulting from the phase of the applied voltage. The possible small departures from the exactly

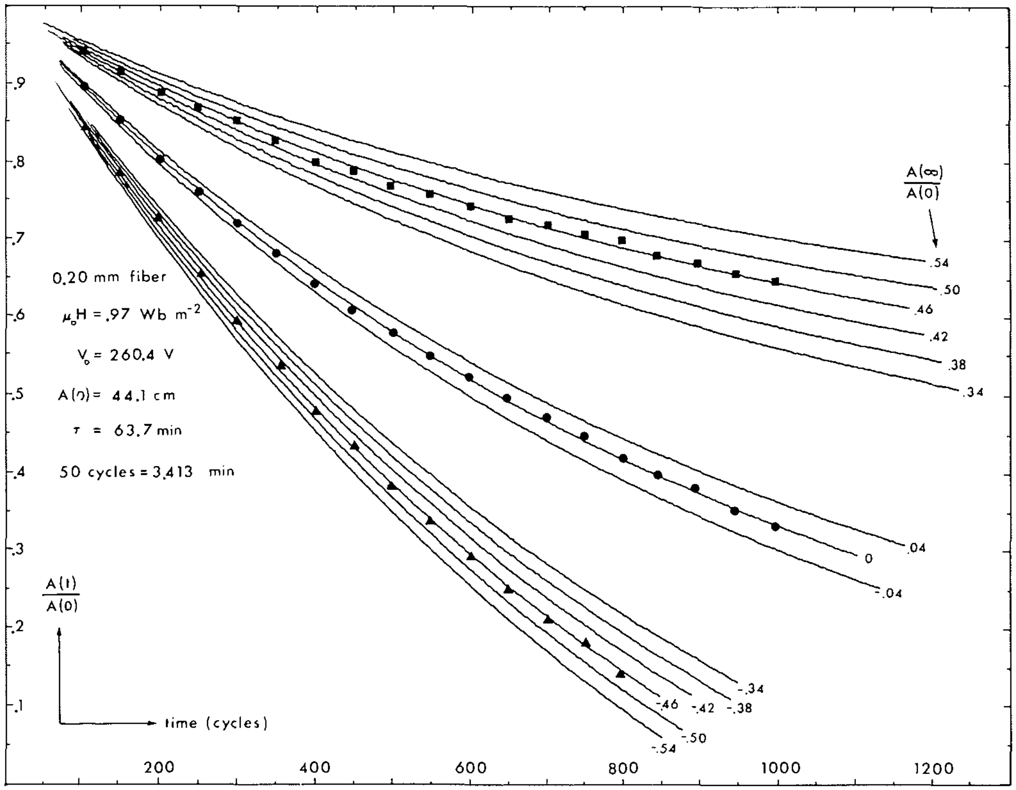

FIG. 6. Transient measurements.

assumed situation $\phi = 0$ or $\phi = \pi$ can be analyzed by remarking that, from [10], in the neighborhood of $t = 0$ the peaks of [9] still occur at $\omega t/\pi$ = integer, whereas for $t = \infty$ they happen a $(\omega t + \phi)/\pi$ = integer. Consequently, the actual envelope of [9] starts as $\hat{\alpha}_1(t) = \alpha_0\, e^{-t/\tau} + (T_0/\delta\omega)\cos\phi[1 - e^{-t/\tau}]$ and ends as $\hat{\alpha}_2(t) = \alpha_0 \cos\phi\, e^{-t/\tau} + (T_0/\delta\omega)[1 - e^{-t/\tau}]$. During the main measurements we were able to set the phase of the applied voltage with accuracy not less than $\Delta\phi = 0.1$ rad ($\cos\phi > 0.995$) and, therefore, the corresponding estimated error due to this cause was less than 0.5%.

Main Measurements

The existence of the Abraham force may be qualitatively determined by simply setting some initial amplitude $A(0)$ for the mechanically oscillating torsional system and observing the decay of the amplitude as in Fig. 6. The effect of applying a voltage across the ceramic in the presence of a perpendicular magnetic field can be readily seen. Depending upon the phase of the applied torque the decay curve is shifted either up or down. A family of exponentials using $A(\infty)/A(0)$ as a parameter may be drawn by computer, using equations [16], [17], and [18], and superimposed on the plot of the measured amplitude decay. It is seen that the observed amplitude decay does follow the calculated curve to within about $\pm 5\%$ and, therefore, allows estimation of $A(\infty)$. The degree of error is the result of two effects: the existence of any disturbance which perturbs the system temporarily and the variation of τ at some intermediate amplitude. The net result is a shift in the decay to another curve specified by a slightly different $A(\infty)/A(0)$. Since the final amplitude $A(\infty)$ will remain the same, this is equivalent to starting the oscillation at some slightly different value of $A(0)$. Further verification of the Abraham force was conducted using this 'transient observation' method by reversing the polarity of the magnetic field and finally by changing the magnitude of the applied electric and magnetic fields. The results were in agree-

TABLE 1. The 'steady state' method

$\omega/2\pi$ (Hz)	$\mu_0 H$ (Wb m^{-2})	V_0 (V)	$A(\infty)$ (cm)	τ (min)	Remarks
0.3836	0.97	260.5	10.1 ± 0.1	36.5(±2)	This τ value is the mean of 32.4 and 40.5 obtained respectively before and after the measurements of $A(\infty)$ which lasted 3 days.
0.3836	0.97	156.3	6.4 ± 0.1	36.5(±2)	
0.3836	0.97	83.4	3.35 ± 0.1	36.5(±2)	
0.3836	0.97	213.5	9.7 ± 0.1	40.5 ± 1	—
0.2448	0.97	260.5	18.1 ± 0.1	62.0 ± 1	Film method
0.2448	0.97	156.3	9.5 ± 0.1	61.3 ± 2	—
0.2448	0.776	260.5	14.0 ± 1	64 ± 4	Mean of two sets of different measurements
0.2448	0.776	156.3	7.5 ± 1	53 ± 2	—

ment with that expected from [16] to [19] but because of the observed experimental difficulties already mentioned, namely, any small but uncontrollable disturbances and the possibility of variation of τ, the calculated values of $A(\infty)$ were up to 10% in error.

One may obviously let the system oscillate sufficiently long that the amplitude approaches the steady state value $A(\infty)$. However, if one selects an initial peak to peak amplitude $A(0) = A(\infty) \pm 1$ cm, it is seen from [16] that after a time interval $\Delta t = 3\tau$ (about 3 h) the steady state swing is practically achieved with an error of less than $[A(\infty) - A(0)]\,e^{-3} \approx 0.5$ mm (the scale readability limit).

With surprise we found that in some instances this method gave two different and well defined scale readings for $A(\infty)$. Although the corresponding maximums of τ were, in fact, within ±5% of the mean value, they caused a lot of trouble: For example, if the three hours steady value of $A(\infty)$ was 7.6 cm, in a further half hour it might change to 6.9 cm to come back to the initial figure one hour or so later. Thus, τ needed to be measured immediately for each $A(\infty)$ to account for any change in the properties of the tungsten fiber. Logarithmic decrement of the unforced decay curve was the method used to measure τ. From [18] one obtains:

$$[25] \qquad \tau^{-1} = \frac{1}{t_2 - t_1} \ln \frac{A(t_1)}{A(t_2)} \simeq \frac{1}{t_2 - t_1} \frac{A(t_1) - A(t_2)}{A(t_2)}$$

where the last approximation could be used for small intervals $t_2 - t_1$. To make the readings of $A(t)$, two observers were seated 3 m from the scale. By using a powerful magnifying glass each observer could record the peak amplitude of the laser spot on his respective side every 10 or 20 cycles. In this way unnecessary movement of the observers was minimized and the suspended system was not disturbed by motion of the air or temperature effects. As an alternative, a 50 frame/s cine camera operated from outside the laboratory was used to record the motion of the laser spot. Individual frames were then viewed in a film analyzer; however, the accuracy was only slightly better than that obtainable using the two observer method.

Consequently, using this method, the procedure was (1) to set the voltage V_0 and the magnetic field $\mu_0 H$ to the required values (vacuum was maintained at 10^{-5} Torr); (2) to set an initial amplitude $A(0)$ within 1 cm of the predicted value of $A(\infty)$ by applying a small rotational force to the suspended system; (3) to record $A(t)$ at half hour intervals over a period of four hours from outside the laboratory through a viewing window to eliminate any disturbance of the system; (4) to immediately disconnect the voltage and, with the ceramic terminals shorted, measure the unforced time constant τ in the region of $A(\infty)$. The actual value for τ was obtained by evaluating [25] either numerically or graphically.

It must be emphasized that due to the sensitive nature of the system used and duration of each run, measurements were generally made in the late evening and early morning: At other times, normal building traffic increased the noise in the system. One other problem encountered was electrostatic charging of the plexiglass window which affected the τ measurements. This was, however, eliminated by placing an α radiation source (^{241}Am) inside the vacuum chamber.

The results using the steady state method are

TABLE 2. Final results

$\omega/2\pi$ (Hz)	$\mu_0 H$ ($\mathrm{Wb\ m^{-2}}$)	V_0 (Volts)	τ (min)	$A(\infty)$ (cm)	T_0^{calc} ($\times 10^{10}$ Nm)	T_0^{obs} ($\times 10^{10}$ Nm)	Error (%)
0.3836	0.97	260.5	36.5	10.1	4.36	4.15	−5
0.3836	0.97	156.3	36.5	6.4	2.62	2.65	+1
0.3836	0.97	83.4	36.5	3.35	1.40	1.39	−0.7
0.3836	0.97	213.5	40.5	9.7	3.58	3.71	+3.6
0.2448	0.97	260.5	62.0	18.1	2.78	2.89	+4
0.2448	0.97	156.3	61.3	9.5	1.67	1.53	−9
0.2448	0.776	260.5	64	14.0	2.23	2.16	−3
0.2448	0.776	156.3	53	7.5	1.34	1.40	+4
0.2448	0.97	260.4	63.7	19.8	2.78	3.07	+10

given in Table 1, where the two recorded frequencies correspond to tungsten fibers of 0.25 mm and 0.20 mm in diameter.

It may be noted from these tabulated data that the 'Q' of the torsional pendulum was, from [8], in excess of 1500. The assumption in the theory following [7] is therefore valid.

Final Results and Conclusions

Using the measured values of the system parameters as reported, [23] and [24] become:

$$[26] \quad T_0^{\mathrm{obs}} = (3.857 \pm 0.4) \times 10^{-7} \frac{A(\infty)}{\tau} \omega \text{ Nm}$$

$$[27] \quad T_0^{\mathrm{calc}} = (6.95 \pm 0.3) \times 10^{-13} V_0 \omega \text{ Nm}$$

From the measurements given in Table 1, the final results using [26] and [27] are summarized in Table 2. For comparison, results derived from the transient method in Fig. 6 are added at the bottom of Table 2.

The total error limit of the experiment can easily be obtained from [26], [27], and Table 1. Therefore, in conclusion, it is possible to state that, for the $BaTiO_3$ specimen, the measured torque agrees with that one calculated from the Abraham density force within the overall experimental error limit of about 10%.

Acknowledgments

The authors wish to thank the following staff members for their help and advice: Professors C. R. James, R. P. W. Lawson, R. W. King, H. J. J. Seguin, and J. Tulip. A special word of appreciation is due to the following technical staff members: B. W. Arnold, K. Doerrbecker, G. Fij, J. J. George, E. Gomez, and R. A. Schmaus.

Thanks is also extended to the Nuclear Research Center for providing the sample of ^{241}Am. Acknowledgment is made to the National Research Council of Canada for the award of a grant.

ABRAHAM, M. 1909. Rend. Cir. Mat. Palermo, **28**, 1.
BREVIK, I. 1970. Mat. Fys. Medd. Dan. Vid, Selsk. **37**, No. 13, p. 1.
EINSTEIN, A. and LAUB, J. 1908. Ann. Phys. **26**, 541.
JAMES, R. P. 1968. Ph.D. Thesis, Dept. of Electrical Engineering, Stanford University.
MARX, G. and GYORGYI, G. 1954. Acta Phys. Hung. **3**, 213.
MINKOWSKI, H. 1908. Nachr. Ges. Wiss. Goettingen, Math.-Phys. Kl., p. 53.
PAULI, W. 1958. Theory of relativity (Pergamon Press Ltd., N.Y.), pp. 110, 216.
WALKER, G. B. and LAHOZ, D. G. 1975. Nature, **253**, 339.
ZENER, C. M. 1948. Elasticity and anelasticity of metals (The University of Chicago Press, Chicago).